TRANSPORT
ISSN 1648-4142 / eISSN 1648-3480
2015 Volume 30(2): 194–201
doi:10.3846/16484142.2015.1045937

INVESTIGATION OF THE INFLUENCE OF A-PILLAR ON PASSIVE SAFETY OF A VEHICLE IN CASE OF ROLLOVER

Vytautas Dzerkelis, Žilvinas Bazaras, Vaidas Lukoševičius

Dept of Transport Engineering, Kaunas University of Technology, Lithuania

Submitted 6 March 2014; resubmitted 28 August 2014; accepted 9 January 2015

Abstract. The need for the means ensuring passive safety of a vehicle is becoming increasingly emphasized in the area of transport engineering. This area becomes particularly relevant when restoration of the damaged load bearing structures in vehicles is concerned. When performing restoration and modification of the vehicles according to specific needs or repairing them after traffic accidents, the lack of norms giving formalized determination of passive safety and recommendations for its assurance becomes obvious. Computational model of the roof structure developed in LS-DYNA is presented, the weld intended for the structure joints is modelled, and residual stresses due to welding process are taken into account, the most effective model of weld location for A-pillar is selected and the influence of A-pillar on the strength of vehicle's roof structure is determined in case of quasi-static compression.

Keywords: vehicle; roof; body; welding joints; A-pillar; rollover; residual stresses; passive safety.

Introduction

More than 40000 people die and about 1.6 million people are injured in road accidents in the European Union (Rivara *et al.* 2003; Jehle *et al.* 2007; Fréchède *et al.* 2011). The number of rollover accidents has significantly increased recently. A lot more vehicle occupants are injured in rollover accidents than in head-on or side collisions. While rollover car accidents make up about 4% of all car accidents, 20 % of fatal accidents involve rollover (Eastman *et al.* 2004). Head and neck injuries are among the most common injuries associated with rollover accidents (Yoganandan *et al.* 1989). Such traffic accidents are very different from front, side (Keršys *et al.* 2011) or back collisions. They are complex phenomena influenced by a great variety of factors.

Automobile manufacturers, transport safety institutes and universities have conducted a number of studies aimed at mitigating the damage caused by rollover of a vehicle (Cho, Han 2012). Identification of actual crush-resistance of roof structure is difficult due to circumstances acting during the traffic accident (Stephenson 2012). In about 90% of the accidents, a vehicle rolls over more than once. Injuries are mainly caused by roof structure being too week, people falling out of the windows, and unfastened seatbelts (Cooper *et al.* 2001; McGregor *et al.* 2010). The latter two causes were identified by vehicle safety specialists around 1960.

Researchers (Cooper *et al.* 2001) came to the conclusion that the average rollover roof deflection may reach ~152 mm. The analysis has shown that large roof deflections during rollover significantly reduce the survival area for the passenger's head, increase the possibility of injury, and contribute considerably to severity of injuries. Researchers analysing rollover accidents have identified 6 main rollover cases (Table 1). These are further categorized by the nature of roof structure deformation and deformed structural members (Fig. 1).

Table 1. Occurrence distributions of roof crush modes (n = 161) (Gugler, Steffan 2006a, 2006b)

Roof crush mode	Distribution of occurrence [%] (n)
1	12 (19)
2	4 (6)
3	27 (44)
4	8 (13)
5	12 (20)
6	2 (4)
None	24 (38)
Others	11 (17)
Total	100 (161)

Corresponding author: Vytautas Dzerkelis
E-mails: *vytautas.dzerkelis@ktu.lt; vytautasdz@gmail.com*

Taylor & Francis
Taylor & Francis Group

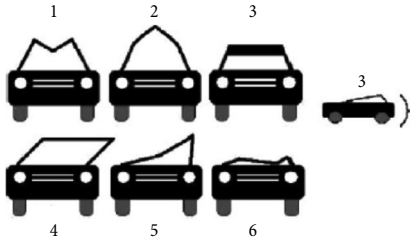

Fig. 1. Main roof crush modes (Gugler, Steffan 2006a, 2006b)

In 27% of rollovers (Fig. 1, pos. 3), roof structure deflection occurs behind the front seats. This means that roof pillars become completely deformed. This type of roof deformation reduces the survival area by as much as 100%. In about 12% (Fig. 1, pos. 1) of rollovers, front roof header is subject to deformation, whereas in 12% (Fig. 1, pos. 5) of the cases, both front roof header and A-pillar become deformed. Injuries in case of this type of roof deformation depend greatly on passengers' position in the vehicle.

As a result of the insufficiently strong structure, about 75% of vehicles undergo significant roof deformations during road accidents (Chen *et al.* 2007).

The case in Fig. 1, pos. 6 is characterized by 100% deformation of roof structure and the highest risk of injury. In case of rollover in Fig. 1, pos. 2, A-pillar of the roof is deformed in an outward direction of the vehicle. In 24% of rollovers, roof deformation is avoided (Mao *et al.* 2007).

Researchers Nash and Paskin (2005) have studied 273 rollover cases, in the majority of which main vehicle roof structure members have been found to be too weak. Joint between the A-pillar, roof side member and front headers has been identified as one of the weakest points. Further studies have demonstrated that during the first roof-to-ground interaction, A-pillar and front header members are subject to the greatest load (Chen *et al.* 2007). Digges (2001) has pointed out that the situation involving 180° rotation in the air and landing on the A-pillar is particularly dangerous. Friedman and Chng (1998) have determined that minor injuries are only characteristic for cases, where average roof deflection is less than 102 mm. Certain studies (McGregor *et al.* 2010) emphasize the advantages of high-strength steel alloys in load-bearing structures.

Vehicle operation and design practice shows that the damage of roof structure and A-pillar joint is critical. This generally relates to lack of adequate consideration of structural strength of the joint for technological, logical, economic or configuration reasons. The analysis of vehicle rollover accidents has shown very complex nature of loads acting on this joint. Finite Element (FE) modelling of such complex structures as joint between vehicle roof and A-pillar usually allow for certain simplification of the model by isolating certain members and maintaining boundary conditions, thus reducing the time of solution time without any compromise to accuracy of the solution. Several calculation schemes can be applied for the same structure depending on the operating conditions simulated by the model. Hence, simplified calculation schemes are more preferable at the initial stages, even if they involve very rough idealization of typical operating conditions of a vehicle roof structure. The objective of this stage of roof structure study was to assess residual stresses as a result of welding processes during repair works and analyse the influence of roof members on the overall strength of the structure by building a FE model of the weld. Following formalization of the initial solutions, it becomes possible to identify how the strength of the A-pillar structure is influenced by the difference between various mechanical characteristics of materials used for the weld vs. mechanical characteristics of the structural material, and to determine the most effective weld location mode in the A-pillar.

1. Review of Rollover Test Methods

Strength and energy absorption capacity of structural members in vehicles is very important in predetermining and restricting compressive forces on the roof structure. Rollover tests used to lack accuracy and information at the very beginning (De Haven 1952), and have continuously been undergoing improvements and revision.

As the number of rollover accidents has been increasing, more tests and their systems providing the most representative rollover situation possible and guaranteeing passive safety of the structure have been emerging. Besides additional methods involving ramps or other obstacles and moving vehicle, manufacturers usually carry out three main rollover tests: static and two patented dynamic tests – Controlled Rollover Impact System (CRIS) and Jordan Rollover System (JRS). Static Roof Crush Test is the most common method applied to vehicle roofs (Fig. 2).

Federal Motor Vehicle Safety Standard (FMVSS) has established the requirement for the roof structure of light-duty vehicles to withstand the load exceeding the weight of the vehicle by 3 g, with static deflections not exceeding 125 mm. Same requirements of the standard apply to light-duty trucks and vans weighing 2722 kg or less. This is the simplest and the most common test method used for vehicle roof structures (Mohan *et al.* 2006). This method is characterized by the following attributes:

– use of rigid heavy-duty metal plate $L_1 \times L_2$ (1829×762 mm), w = 254 mm;

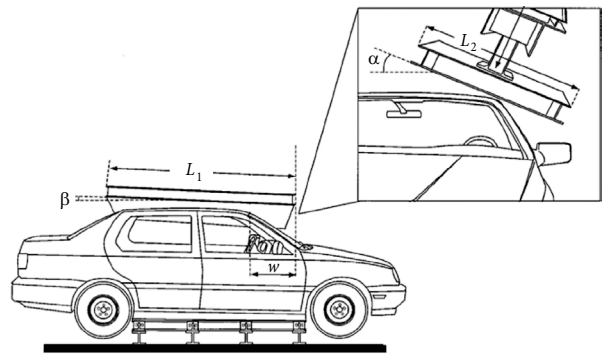

Fig. 2. Static roof crush testing (Mohan *et al.* 2006)

– the plate is directed along the tested object, with the horizontal plane inclined at $\beta = 5°$;
– lateral angle with the horizontal equal to $\alpha = 25°$ (Fig. 2).

It has been demonstrated by various research works that, considering current FMVSS 216 test procedure, static roof crush resistance of vehicles depends heavily on the radius of curvature of the windscreen and direction of load. The moment of crack of the windscreen, followed by noticeable reduction of roof structure strength, contributes greatly to the results (Mao *et al.* 2007).

It has been determined that the actual crush resistance of a vehicle roof is considerably lower than declared during FMVSS 216 tests. Roof structure is considered to be subject to only 73% of the actual accident load during tests under FMVSS 216 instructions (Brumbelow *et al.* 2009). It has been determined that at least twice as high Strength-to-Weight Ratio (SWR) should be used and loading angles should be revised. Strength of roof structure – with or without windscreen – should also be defined (Friedman, Nash 2003).

Besides the mentioned roof structure test, another test, offering considerably more accurate replication of possible crush of roof structure and vehicle kinematics, has been proposed (Chen *et al.* 2007). Its distinctive feature is shifting direction of load during the test. When the vehicle roof structure is subject to compressive forces, the plane of loading adapts to the shape of the deformed body, thus providing a relatively realistic case of roof deformation. The test begins at 6° angle between the body and the pavement. Loading plate is guided at 8° angle with the roof plane. The plate rotation angle changes throughout the test (Fig. 3).

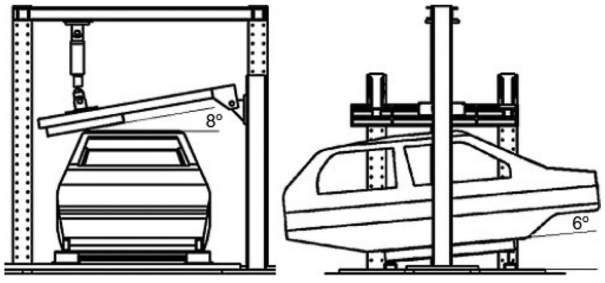

Fig. 3. Roof crush test set-up (Chen *et al.* 2007)

The amount of absorbed energy E is determined by measuring turning moment and turn angles during the test (Chen *et al.* 2007):

$$E = \int_{\phi 0}^{\phi 1} M(\phi) d(\varphi), \quad (1)$$

where: M – moment [Nm]; ϕ – turning angle [rad].

2. Construction and Validation of Computational Model

To accelerate calculations, all members having no effect on rigidity of vehicle roof structure have been removed from FE models of vehicles. Depending on the body members under load, members having no effect on final calculation results have been removed from the simplified model of load-bearing structure (Fig. 4).

Three members can usually be found in a typical roof structure (Fig. 5): A-pillar (a), roof front header (b) and roof side rails (c). Analysis of simplified structures has confirmed the assumption that in case roof structure is subjected to bending load, these roof members usually tend to undergo radical deformations.

A-pillar has been determined to be the first to lose its bending strength, followed by roof front header and side rails deformation. It is natural for the first two members to be subjected to the greatest loads and become the weakest point of the roof structure compared to roof side rails. The latter are usually reinforced with view towards possible side collision with an obstacle.

In order to recreate in details the influence of roof members of a light-duty vehicle on the overall strength of the structure, computational method of the tested vehicle devised by researchers (NCAC 2008; Nassiopoulos, Njuguna 2011) has been used. The latter has been chosen, as it has already been validated in cases of front and side collision.

Calculations have been carried out for the following three cases: with upper section of A-pillar, front header, and roof side rails above the front doors eliminated. The results of the computational modelling are presented in Fig. 6.

In order to determine the influence of load-bearing members in modern vehicles and the latest grades of steel used in vehicles on the strength of roof structure, steel grades satisfying mechanical characteristics (Steel Works 2015) presented in Fig. 7 have been chosen for vehicle body members. Similar tendency of body member deformation in a tested vehicle has been registered when using different materials for roof members and applying quasi-static loads (Fig. 8).

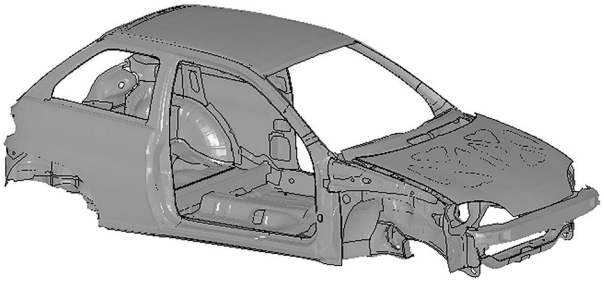

Fig. 4. Simplified structure of the tested vehicle (Schmitt 2009)

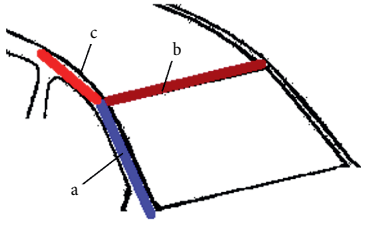

Fig. 5. Simplified typical roof structure: a – A-pillar; b – roof front header; c – roof side rails (Dzerkelis, Bazaras 2013)

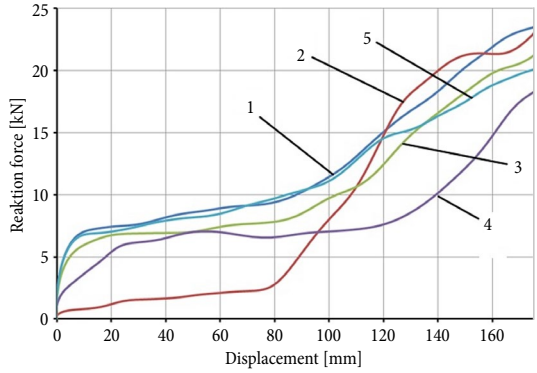

Fig. 6. Pillar reactions of a standard vehicle: 1 – full structure; 2 – without A-pillar; 3 – without front header; 4 – without side rail; 5 – without B-pillar

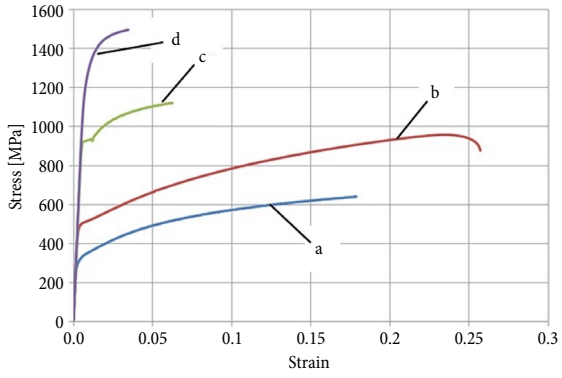

Fig. 7. Steel alloys: a – DP 500; b – TRIP 780; c – DP 980; d – MS 1400

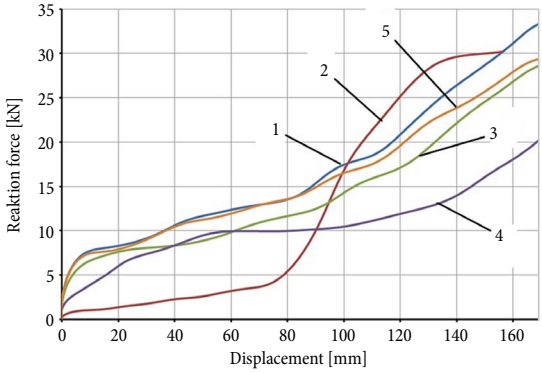

Fig. 8. Reactions of the support in a modified vehicle: 1 – full structure; 2 – without A-pillar; 3 – without front header; 4 – without side rail; 5 – without B-pillar

Analysis of the presented data has shown that elimination of A-pillar reduces the strength of roof structure by 78%. This difference is noticed at the very beginning of loading up until 75 mm roof angle displacement. Support reaction increases under further loading. At this point, the influence of B-pillar on the strength of the structure becomes apparent. This has been found by elimination of the upper section from the structure. The graph shows that in case displacement exceeds 80 mm, the curves of change of loads on the intact body vs. the body without B-pillar split, and reaction of the support noticeably decreases. After front roof header has been eliminated from the load-bearing roof structure, reaction of the support in such structure vs. full structure is noticeably lower, whereas in case of 40 mm roof angle displacement, the reaction reduces by 18% on average. After elimination of side roof structure members from the structure, the reaction of the support at the beginning of loading up until 55 mm displacement has been found to be lower by 14% on average compared to full structure, and in case of 127 mm displacement, the reaction of the support has reduces by 45%.

In case of potentially repaired structure, welds are additionally integrated into A-pillars in the computational model. Welds are located in the most effective mode determined during the analysis of the influence of A-pillar weld location on the strength of the pillar. During the analysis of crush resistance, it has been noticed that load reaction is similar to the case where an intact structure is used, and reduces by 4.8% on average at 122 mm displacement only.

3. Construction of Computational Model of A-pillar and Weld

In order to ensure passive safety of a vehicle during rollover, roof crush resistance has been calculated. A-pillar of the vehicle and the influence of welds made during the recent repair and their location on the structural strength have been analysed (Fig. 9).

One end of a 0.56 m long beam is fitted by restricting all degrees of freedom, while another end is subjected to load by an ideally solid body of a predetermined mass and speed (by solving a dynamic problem) or axial displacement of the latter (by solving a quasi-static problem).

A-pillar is usually comprised of 3 sections (Fig. 10): outer section attributed to A class surfaces, middle section and inner section. In the computation model, these sections of structure were joined by simulating spot welding every 50 mm. Welding spot diameter – 6 mm.

In practice, during replacement of vehicle roof, A-pillar is joined to allow overlapping of elements of the replaced parts. A 'window' is cut out in the upper section of A-pillar to connect the middle section. The latter is usually welded in the centre of the 'window'.

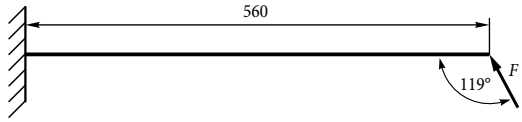

Fig. 9. Simplified loading scheme of A-pillar

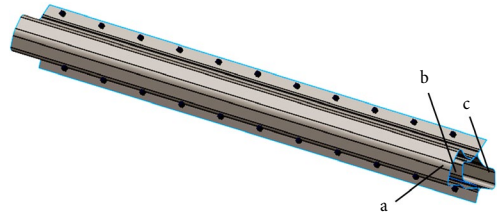

Fig. 10. A-pillar with spot welding: a – outer section, b – middle section, c – inner section

Middle section of the pillar is welded at the distance of approximately 100 mm from the welding spot of inner sections. In order to analyse the structure by building on these recommendations, weld location on the sections of members, their location in relation to each other have been pre-determined and four types of models have been developed (Fig. 11).

In Type I model, sections of the pillar are joined and a 'window' is designed 67.5 mm from the fixing point. Middle sections would be welded in the middle of the 'window' of the upper section. Inner section of A-pillar would be connected 185 mm from the fixing point. In Type II model, upper sections of A-pillar are connected and a 'window' is designed in the middle of the structure. Inner section would be connected 180 mm from the welding point of the middle section, closer to the fixing point. Type III model is equivalent to the second model, except for the joint of the inner section, which is 365 mm from the welding point of the middle section, closer to the location where additional load is applied. In Type IV model, pillar sections are joined and the 'window' is designed at a distance from the fixing point. Welding location of the middle sections is modelled in the middle of the 'window' of the upper section. Inner section of the pillar would be connected 360 mm from the fixing point.

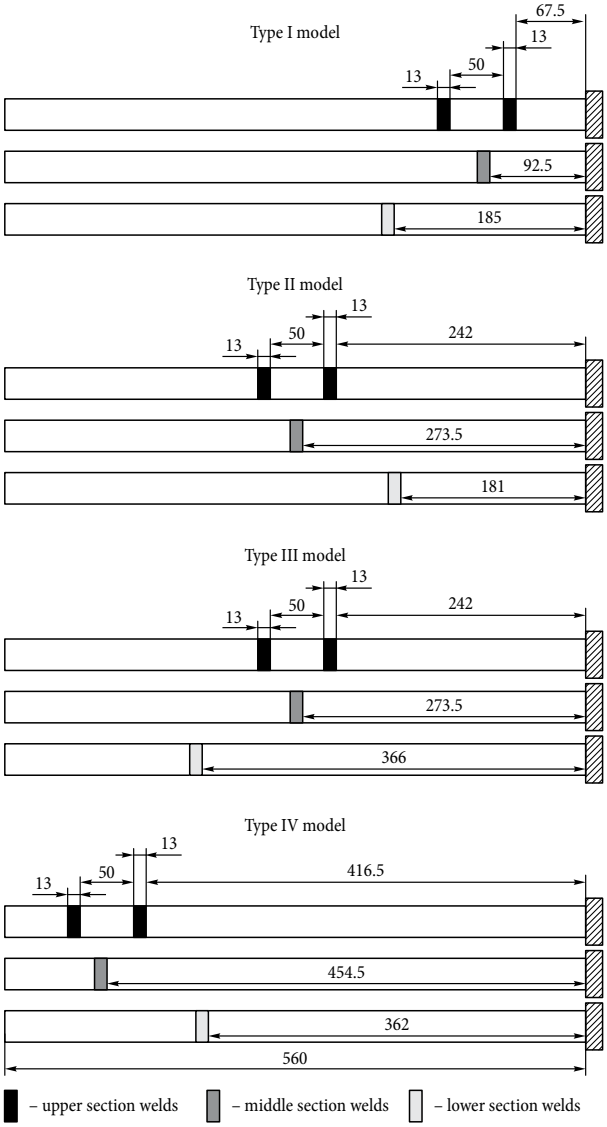

Fig. 11. Weld location options (Dzerkelis *et al.* 2012b)

Vickers test (Bazaras, Kalpokas 2002; Bazaras *et al.* 2001) performed to verify hardness of the weld by experiment has determined yield strength σ_y, i.e. the minimum stress, at which deformation of the sample increases under nearly constant load, and yield point σ_e – the maximum stress, at which no residual deformation exists in the sample:

$$\sigma_y = \frac{H_V}{C} \cdot 0.1^n; \tag{2}$$

$$\sigma_e = \frac{H_V}{2.9} \cdot \left(\frac{n}{0.217} \right)^n, \tag{3}$$

where H_V – hardness by Vickers [MPa]; C – constraint factor of elasticity (constant equal to 3); n – exponent of load strength (for metals, where H_V = 2000–3000 MPa, the exponent equals to 0.12 or 12%).

Weld is modelled in the welding location based on distribution of residual stresses at the points of the control line, calculated under Vickers principle (Fig. 12).

Fig. 12 shows that residual stresses occur at joint of the members due to thermal processes. 3 characteristic sections of weld could be identified by analysing the presented graph. In section 1, the maximum value of residual stresses reaches 205 MPa. The width of this section is 2–3 mm (or 1–1.5 mm from the centre of the weld on both sides). In section 2 of the weld, the maximum value of residual stresses reaches 282 MPa, with the width equal to 2–3 mm. Section 3 is located 4 mm from the centre of the weld, with the maximum residual stresses reaching 190 MPa.

For this paper, LS-DYNA V.971 FE application has been used to simulate elements undergoing deformation.

FE model of A-pillar of adequate structure and geometrical parameters has been chosen based on geometrical paramters of the vehicle tested during natural experiments for simulation of quasi-static experiments. Each lower node of the tested A-pillar was tightened at 6 degrees of freedom. Deformation of the analysed structure was caused by action of an absolutely rigid body 'RIGID BODY' on the structure. It was assumed that the

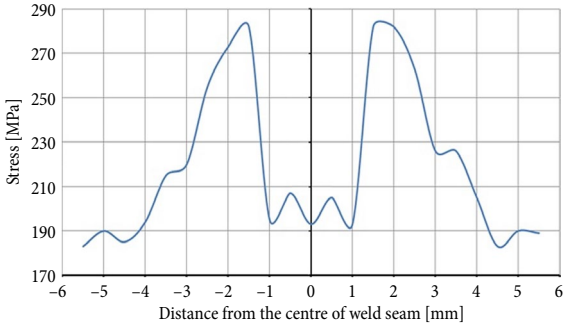

Fig. 12. Distribution of residual stresses at points of the control line (Dzerkelis *et al.* 2012a, 2012b)

point of possible contact with the pavement at rollover had been made of absolutely rigid material, without any consideration of elasticity and shock absorption characteristics of the surface. In order to solve the quasi-static task relating to the plate elements, command 'BOUNDARY_PRESCRIBED_MOTION_RIGID' was used to preset the constant movement speed in vertical direction *y*, maximum possible deflection. Command 'CONTACT_AUTOMATIC_SINGLE_SURFACE' was used for simulation of element surfaces that came into contact with each other at deformation.

Command 'INITIAL_VELOCITY_RIGID_BODY' was applied to solve the task of shock energy absorption by applying the method. Since the structure was fixed during the chosen solution, and deformations were caused by the rotating absolutely rigid plate, concentrated mass 'MASS' was added to the centre of area of contact between the plate and the structure in order to maintain the component of possible vehicle inertia in the obtained results.

Spot-weld joints were created in the model by commands 'SEACTION_BEAM' and 'MAT_SPOT_WELD'. Mechanical characteristics and geometrical parameters of the material were preset for connections. Each spot-welded joint in the model was comprised of a rod element connecting two joints.

Shell FEs were used for simulation of buckling of the thinwalled structural elements in this work. Linear, four-node flat Belytschko-Tsay shell FEs calculated by Mindlin-Reissner thick-walled plates theory, with 1 integration point in the plane of the element and 5 integration points in thickness stretch of the element, were chosen in the work for assessment of variation in thickness of the element during deformation. Zero-energy effect of deformation (Hourglasing) may have occurred in the model in case deformation speed was increased, and additional control was preset for the elements to avoid such effect.

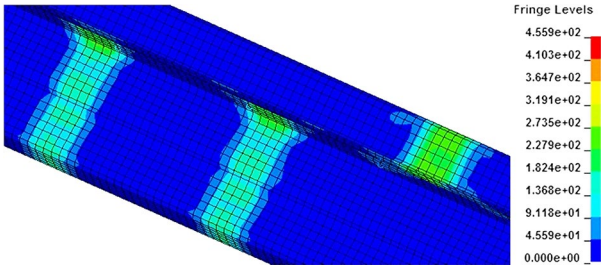

Fig. 13. FE model and residual stresses of the seam welding

Based on the obtained results, FE model with residual stresses has been built (Fig. 13).

4. Quasi-Static Bending of Welded Roof A-Pillar

Quasi-static analysis has shown that the influence of seam weldings on a structure made of members produced from DP 500 and TRIP 780 steel is minor compared to an intact structure, i.e. no weakening of structure during quasi-static loading has been determined. In case of DP 500 steel, the maximum reaction of support is 5000 N, at 95 mm displacement of the end of structure under load. Buckling of the structure starts at 150 mm displacement of the end under load and at 3500 N reaction of support.

In case of TRIP 780 steel, the maximum reaction of support of 6800 N has been registered at 80 mm displacement of the end under load. The structure is stronger by 36% compared to a structure made of DP 500 steel.

At loading of DP 980 steel structure, it has been noticed that changes occur, where mechanical characteristics of weld material are lower than mechanical characteristics of the structure (Fig. 14). Compared to reaction of support in an intact structure, Type I structure joint model is the weakest. The maximum load is 11000 N and 2% higher than load on an intact structure at 92 mm displacement of the end under load. It has also been determined that if an intact structure is subjected to load, the maximum reaction of support is 11500 N at 66 mm displacement. Having compared the reaction of support in a repaired structure and structure joined under Type I joint scheme, it has been noticed that reaction of support in a repaired structure is 4.4% lower compared to the intact structure. Bending strength of all the analysed models is the same until 6000 N reaction of support and 20 mm displacement are reached.

As displacement of the structure end under load increases to 66 mm, reactions of support in Type I and II models reduce by 2.8% and 14.4% on average com-

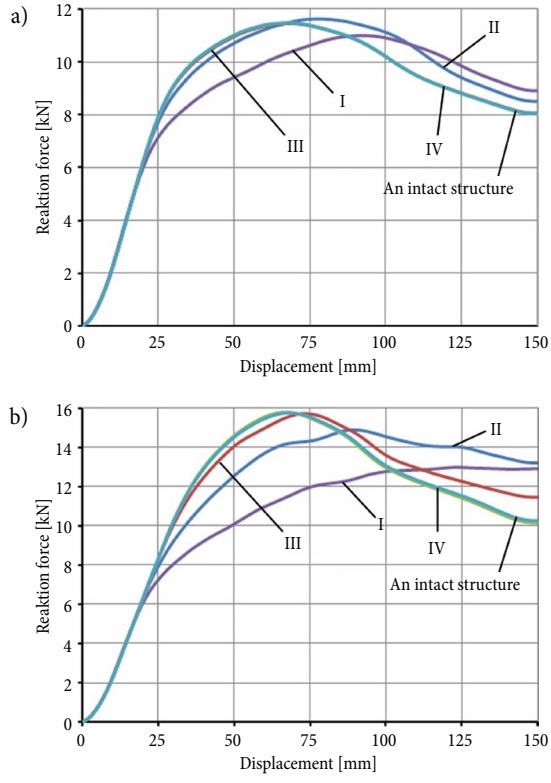

Fig. 14. Reactions of A-pillar support depending on the steel grade (I – Type I model; II –Type II model; III –Type III model; IV –Type IV model): a – DP 980; b – MS 1400

pared to an intact structure. At 66 mm displacement, the load on intact structure reaches the maximum value of 11500 N that decreases by 23% at 127 mm displacement.

Type II joint structure is subject to the maximum 11600 N load at 78 mm displacement of the end under load. In this case, the load is 3% higher than on an intact structure. At 127 mm displacement of the structure end under load, reaction of the support decreases by 19.5%; however, compared to the load on an intact structure, the latter is higher by 6%.

Calculation results have suggested that the better mechanical characteristics of structural materials and the bigger the difference to mechanical characteristics of the weld, the greater the importance of the tested seam welding methods for crush resistance of structure (Fig. 15). 6000 N reaction force is achieved for all the analysed models at 20 mm displacement. As the displacement increases, the value of reaction of support sets at 12900 N. During bending of Type II model, reaction of support reaches the maximum value of 14900 N at 90 mm displacement. As displacement increases to 127 mm, the value of load decreases by 6%. In Type III model, the maximum value of load reaction at 74 mm displacement is 15600 N. With the increase of displacement to 127 mm, the load reaction value decreases by 22%. Similar results can be noticed during analysis of the curve of support reaction in Type IV model. The results of the rest of the models demonstrate that at 127 mm displacement, support reactions become higher compared to reaction of an intact structure. Respectively, in case of Type I model, the difference is 13%, II – 22%, III – 6.5%.

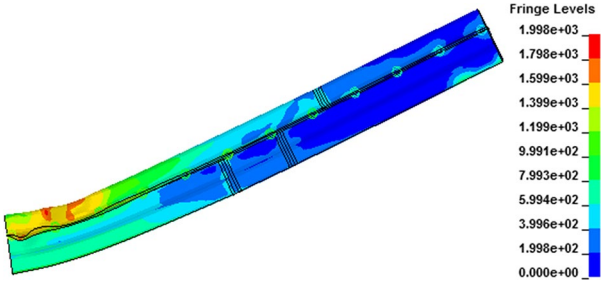

Fig 15. Influence of Type III seam weldings location on distribution of stresses of MS 1400 steel structure

For the analysis of load-bearing structures in complex vehicles and computational schemes, it is preferable to analyse the behaviour of the entire load-bearing structure in case of complex load rather than only to confine to analysis of stress and deformation state of an isolated member and formulation of the criteria of strength, rigidity and energy absorption capacity.

Conclusions

The paper has analysed the influence of roof structure and A-pillar seam welding in roof structure of repaired vehicles on passive safety. Software package LS-DYNA has been used for computation. FE model of A-pillar of a vehicle has been developed, and criteria for crush resistance at various load conditions have been determined. The main advantage of similar computational problem solutions is the possibility to provide a fairly detailed description or analysis of rollover of a vehicle, which is not as easy when using conventional analytical methods.

Analysis of load-bearing roof structure of the vehicle has shown that elimination of A-pillar from roof structure has the greatest impact on crush resistance of the structure. In this case, reaction of support has been estimated to decrease by 78%.

Assessment of differences between mechanical characteristics of steel used in vehicle structures and steel used for seam weldings between structural members during body repair works has shown that the higher and the more different from the weld mechanical characteristics of structural materials are, the deformations of the welded structure are more apparent.

Analysis of the presented cases of weld location has suggested that Type III model is the most effective. Deformation of this model is the closest to the case of an intact structure, where decrease of support reaction is about ~3%.

In order to identify the possibilities of compensation of crush resistance of the structure, computational studies using foam-filled structure and verification of correlation between different results of quasi-static and dynamic deformation are planned to be performed in future.

Acknowledgements

This work has been supported by the European Social Fund within the project 'Development and application of innovative research methods and solutions for traffic structures, vehicles and their flows', project code VP1-3.1-ŠMM-08-K-01-020.

References

Bazaras, Ž.; Kalpokas, J. 2002. Evaluation of residual stresses in welded rails, *Mechanika* (1): 22–26.

Bazaras, Ž.; Markšaitis, D.; Rumša, I. 2001. Suvirintų bėgių siūlų mechaninių savybių įvertinimas, *Mechanika* (4): 13–16. (in Lithuanian).

Brumbelow, M. L.; Teoh, E. R.; Zuby, D. S.; McCartt, A. T. 2009. Roof strength and injury risk in rollover crashes, *Traffic Injury Prevention* 10(3): 252–265. http://dx.doi.org/10.1080/15389580902781343

Chen, T.; Chirwa, E. C.; Mao, M.; Latchford, J. 2007. Rollover far side roof strength test and simulation, *International Journal of Crashworthiness* 12(1): 29–39. http://dx.doi.org/10.1533/ijcr.2006.0156

Cho, Y. H.; Han, B. K. 2012. Roof strength performance improvement enablers, *International Journal of Automotive Technology* 13(5): 775–781. http://dx.doi.org/10.1007/s12239-012-0077-5

Cooper, E.; Moffatt, E.; Curzon, A.; Smyth, B.; Orlowski, K. 2001. Repeatable dynamic rollover test procedure with controlled roof impact, *SAE Technical Paper* 2001-01-0476. http://dx.doi.org/10.4271/2001-01-0476

De Haven, H. 1952. Accident survival – airplane and passenger car, *SAE Technical Paper* 520016. http://dx.doi.org/10.4271/520016

Digges, K. 2001. *Develop Improved Roof Crush Test Procedure: Proposed Research Plan and Milestones*. 4 p. Available from Internet: http://fdnweb.org/santos/files/2014/11/rcrp.pdf

Dzerkelis, V.; Bazaras, Ž. 2013. Research of loads distribution on a car roof elements with changing operating angles, in *ITS 2013: Proceedings in Intelligent Transportation Systems 2013 (Virtual Conference)*, 26–30 August 2013, Žilina, 53–56. Available from Internet: http://www.itransport.sk/archive/?vid=1&aid=2&kid=100101-22

Dzerkelis, V.; Bazaras, Ž.; Zelenius, V. 2012a. Investigation of the hardness of the welded joints of the car's construction, Intelligent technologies in logistics and mechatronics systems, in *ITELMS'2012: Proceedings of the 7th International Conference*, 3–4 May 2012, Panevėžys, Lithuania, 62–65.

Dzerkelis, V.; Zelenius, V.; Bazaras, Ž. 2012b. Investigation of car roof a-pillar repair, in *Transport Means–2012: Proceedings of the 16th International Conference*, 25–26 October 2012, Kaunas, Lithuania, 259–262.

Eastman, A. B.; Hoyt, D. B.; Conroy, C.; Erwin, S.; Pacyna, S.; Vaughan, T. 2004. *Rollovers Configuration, Kinematics, and Injury*. The National Highway Traffic Safety Administration (NHTSA). 50 p. Available from Internet: http://www.nhtsa.gov/DOT/NHTSA/NVS/CIREN/2004%20Presentations/1104SanDiego.pdf

Fréchède, B.; McIntosh, A. S.; Grzebieta R.; Bambach, M. R. 2011. Characteristics of single vehicle rollover fatalities in three Australian states (2000–2007), *Accident Analysis & Prevention* 43(3): 804–812. http://dx.doi.org/10.1016/j.aap.2010.10.028

Friedman, D.; Chng, D. 1998. Human subject experiments in occupant response to rollover with reduced headroom, *SAE Technical Paper* 980212. http://dx.doi.org/10.4271/980212

Gugler, J.; Steffan, H. 2006a. *Improvement of Rollover Safety for Passenger Vehicles*. Final Public Report, July 2002 – December 2005. European Community – R&TD-Project – 5th Framework-Programme "Growth". 22 p. Available from Internet: http://www.transport-research.info/Upload/Documents/201003/20100318_180543_7485_Rollover_Final_Public_Report.pdf

Gugler, J.; Steffan, H. 2006b. *Improvement of Rollover Safety for Passenger Vehicles*. Annex I – Final Public Report, July 2002 – December 2005. European Community – R&TD-Project – 5th Framework-Programme "Growth". 192 p. Available from Internet: http://www.transport-research.info/Upload/Documents/201003/20100318_180718_75129_Rollover_Final_PublicReport_Annex.pdf

Friedman, D.; Nash, C. E. 2003. Measuring rollover roof strength for occupant protection, *International Journal of Crashworthiness* 8(1): 97–105. http://dx.doi.org/10.1533/ijcr.2003.0221

Jehle, D.; Kuebler, J.; Auinger, P. 2007. Risk of injury and fatality in single vehicle rollover crashes: danger for the front seat occupant in the "outside arc", *Academic Emergency Medicine* 14(10): 899–902. http://dx.doi.org/10.1197/j.aem.2007.06.029

Keršys, A.; Pakalnis, A.; Lukoševičius, V. 2011. Investigation of occupant fatalities and injuries during the impact of vehicle and road safety barrier, *The Baltic Journal of Road and Bridge Engineering* 6(1): 5–11. http://dx.doi.org/10.3846/bjrbe.2011.01

Mao, M.; Chirwa, E. C.; Chen, T. 2007. Reinforcement of vehicle roof structure system against rollover occupant injuries, *International Journal of Crashworthiness* 12(1): 41–55. http://dx.doi.org/10.1533/ijcr.2006.0157

McGregor, C.; Vaziri, R.; Xiao, X. 2010. Finite element modelling of the progressive crushing of braided composite tubes under axial impact, *International Journal of Impact Engineering* 37(6): 662–672. http://dx.doi.org/10.1016/j.ijimpeng.2009.09.005

Mohan, P.; Nagabhushana, V.; Kan, C.-D.; Riley, J. 2006. *Innovative Approach for Improving Roof Crush Resistance*. LS-DYNA Anwenderforum. 10 p. http://citeseerx.ist.psu.edu/viewdoc/download?doi=10.1.1.208.6539&rep=rep1&type=pdf

Nash, C. E.; Paskin, A. 2005. A study of NASS rollover cases and the implication for federal regulation, in *Proceedings of the 19th International Technical Conference on the Enhanced Safety of Vehicles (ESV)*, 6–9 June 2005; Washington, DC. Paper No. 05-0415, 1–15. Available from Internet: http://www-nrd.nhtsa.dot.gov/Pdf/esv/esv19/05-0415-O.pdf

Nassiopoulos, E.; Njuguna, J. 2011. Finite element dynamic simulation of whole rallying car structure: Towards better understanding of structural dynamics during side impact, in *8th European LS-DYNA® Users Conference*, 23–24 May 2011, Strasbourg, 1–15. Available from Internet: http://www.dynamore.de/de/download/papers/konferenz11/papers/session1-paper2.pdf

NCAC. 2008. *Development & Validation of a Finite Element Model for the 1997 Geo Metro Passenger Sedan*. Technical Summary NCAC 2007-T-008, The National Crash Analysis Center (NCAC). 5 p. Available from Internet: http://www.ncac.gwu.edu/research/pubs/NCAC-2007-T-008.pdf

Rivara, F. P.; Cummings, P.; Mock, C. 2003. Injuries and death of children in rollover motor vehicle crashes in the United States, *Injury Prevention* 9(1): 76–80. http://dx.doi.org/10.1136/ip.9.1.76

Schmitt, A. 2009. *Investigation of Different Roof Strengthening Methods to Gain an Elastically Responding Roof in Static and Dynamic Rollover Tests*, Independent Research, The National Crash Analysis Center (NCAC). 115 p. Available from Internet: http://www.autosafetyresearch.org/pdfs/Thesis_Alexander%20Schmitt.pdf

Steel Works. 2015. *Steel Grades*. Available from Internet: http://www.steel.org/sitecore/content/Autosteel_org/Web%20Root/Research/AHSS%20Data%20Utilization/MS1400.aspx

Stephenson, R. R. 2012. The case for a dynamic rollover test, *International Journal of Crashworthiness* 17(2): 119–124. http://dx.doi.org/10.1080/13588265.2011.625677

Yoganandan, N.; Haffner, M.; Maiman, D.; Nichols, H.; Pintar, F.; Jentzen, J.; Weinshel, S.; Larson, S.; Sances, A. 1989. Epidemiology and injury biomechanics of motor vehicle related trauma to the human spine, *SAE Technical Paper* 892438. http://dx.doi.org/10.4271/892438